ELSEVIER

Journal of Organometallic Chemistry 535 (1997) 33–41

Journal of Organometallic Chemistry

Amine adducts of triarylboroxines: synthesis and characterization of adducts of tri(2-tolyl)boroxine and crystal structures of $(4\text{-}MeC_6H_4)_3B_3O_3$ and $(4\text{-}MeC_6H_4)_3B_3O_3 \cdot$ 4-picoline

Michael A. Beckett [a,*], Gary C. Strickland [a], K. Sukumar Varma [a,1], David E. Hibbs [b], Michael B. Hursthouse [b,2], K.M. Abdul Malik [b]

[a] *Chemistry Department, University of Wales, Bangor, LL57 2UW, UK*
[b] *Chemistry Department, University of Wales, Cardiff, PO Box 912, Cardiff, CF1 3TB, UK*

Received 28 August 1996; revised 25 November 1996

Abstract

Seven 1:1 adducts of the triarylboroxine $(2\text{-}MeC_6H_4)_3B_3O_3$ with *N*-donor ligands (4-picoline, cyclohexylamine, pyridine, 3-picoline, piperidine, isoquinoline, benzylamine) have been prepared by reaction of equimolar quantities of amine and $(2\text{-}MeC_6H_4)_3B_3O_3$ in Et_2O at room temperature. These adducts have been characterized by elemental analysis, melting point, IR spectroscopy and by ^1H and ^{13}C NMR spectroscopy. Room temperature solution ^1H NMR spectra of these complexes suggest that rapid ligand dissociation–recombination exchange processes are occurring. The related compounds $(4\text{-}MeC_6H_4)_3B_3O_3$ and $(4\text{-}MeC_6H_4)_3B_3O_3 \cdot$ 4-picoline have been characterized in the solid state by single crystal X-ray diffraction studies. Solid state ^{11}B MAS NMR results are reported for triarylboroxines $(4\text{-}MeC_6H_4)_3B_3O_3$ and $(3,5\text{-}Me_2C_6H_3)_3B_3O_3$ and for the amine adducts $(4\text{-}MeC_6H_4)_3B_3O_3 \cdot$ cyclohexylamine, $(4\text{-}MeC_6H_4)_3B_3O_3 \cdot$ isoquinoline, $(4\text{-}MeC_6H_4)_3B_3O_3 \cdot$ benzylamine, $(3,5\text{-}Me_2C_6H_3)_3B_3O_3 \cdot$ 4-picoline and $(3,5\text{-}Me_2C_6H_3)_3B_3O_3 \cdot$ morpholine. © 1997 Elsevier Science S.A.

1. Introduction

It is well documented [1–5] that triarylboroxines form adducts with amine ligands and in 1958 Synder et al. [1] proposed that the structure of the $Ph_3B_3O_3 \cdot$ py adduct involved coordination of the pyridine nitrogen atom to one of the boron atoms of the boroxine ring. Burg [6] had earlier proposed similar structures for the 1:1 NH_3 and Me_3N adducts of the trialkylboroxine $Me_3B_3O_3$. Low-temperature- [3] and variable-temperature-NMR studies on the 1:1 adducts of triarylboroxines have revealed that in solution there exists a temperature-dependent fluctuation of the amine between the three boron atoms of the boroxine ring and recently [4] this has been attributed to a low activation energy ligand dissociation–recombination (exchange) process. It has been suggested that the free energy of activation ($\Delta G^{\ddagger}$) of this exchange process for the amine adducts of $(4\text{-}MeC_6H_4)_3B_3O_3$ (**1**) and $(3,5\text{-}Me_2C_6H_3)_3B_3O_3$ (**2**) may correlate with steric interactions with higher values obtained for the more congested species. We were interested to see if this trend would continue and this paper reports on the synthesis and characterization of series of hitherto unreported 1:1 *N*-donor adducts of the more sterically demanding triarylboroxine $(2\text{-}MeC_6H_4)_3B_3O_3$ (**3**). We also report the crystal and molecular structures of the related compounds **1** and $(4\text{-}MeC_6H_4)_3B_3O_3 \cdot$ 4-picoline (**4**). Solid state MAS ^{11}B NMR of **1** and **2** and the amine adducts $(4\text{-}MeC_6H_4)_3B_3O_3 \cdot$ cyclohexylamine (**5**), $(4\text{-}MeC_6H_4)_3B_3O_3 \cdot$ isoquinoline (**6**), $(4\text{-}MeC_6H_4)_3B_3O_3 \cdot$ benzylamine (**7**), $(3,5\text{-}Me_2C_6H_3)_3B_3O_3 \cdot$ 4-picoline (**8**), and $(3,5\text{-}Me_2C_6H_3)_3B_3O_3 \cdot$ morpholine (**9**) are also described in detail.

* Corresponding author.
[1] Current address: Pilkington Group Research, Pilkington Technology Centre, Lathom, Lancashire, L40 5UF, UK.
[2] Also corresponding author.

PII S0022-328X(96)06952-5

2. Results and discussion

2.1. Solid state studies

The molecular structure of the triarylboroxine (4-$MeC_6H_4)_3B_3O_3$ (**1**) as determined by a single crystal X-ray diffraction study, is shown in Fig. 1. It contains a crystallographic twofold axis passing through the O(2), B(2), C(8), C(11) and C(12) atoms. Selected bond distances and angles are given in Table 1. The *p*-tolyl rings and the alternating B_3O_3 boroxine ring are essentially co-planar with bond distances and angles similar to those reported for $Ph_3B_3O_3$ [7]. The B–O distances are identical at 1.383(4)–1.384(4) Å and the boroxine ring angles are, as expected if the bonds were formed from sp^2-hybrid orbitals, close to 120° with the B–O–B angles slightly larger (120.8(4)–121.8(3)°) than the O–B–O angles (117.9(4)–118.8(3)°). Exocyclic bond angles at boron are in the range 119.4(3)–121.1(3)°. Bond angles (116.7(3)–121.6(3)°) and distances (1.373(5)–1.407(5) Å) within the *p*-tolyl rings are within normal ranges with the exception of angles about the *B*-substituted carbon where the C–C–C angles are smaller (116.7(3)–117.3(4)°), but this type of angular distortion in the phenyl substituent is quite common. Steric interactions between the ortho hydrogen atoms and the ring oxygens may be responsible for this distortion. The *p*-tolyl groups are nearly coplanar with the boroxine ring as shown by the torsion angles O(1)–B(1)–C(1)–C(2) of −9.6(5)°, and O(1)–B(2)–C(8)–C(9) of 1.6(2)°. The essentially co-planar arrangement of the *p*-tolyl and boroxine rings enables the molecules to stack efficiently

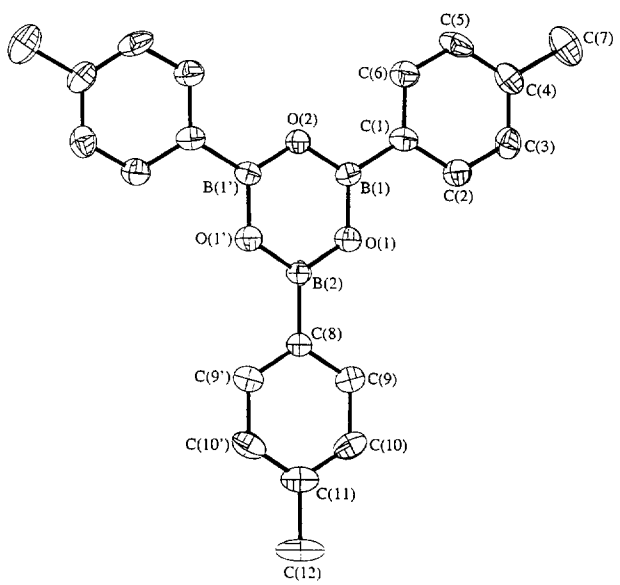

Fig. 1. An ORTEP drawing of (4-$MeC_6H_4)_3B_3O_3$ (**1**) showing the numbering scheme. The primed atoms are generated by a crystallographic twofold axis passing through O(2), B(2), C(8), C(11), and C(12).

Table 1
Selected interatomic distances (Å) and angles (deg) for $C_{21}H_{21}B_3O_3$ (**1**)

Bond lengths			
O(1)–B(1)	1.383(4)	O(1)–B(2)	1.384(3)
O(2)–B(1)	1.384(4)	B(1)–C(1)	1.543(4)
B(2)–C(8)	1.521(6)		
Bond angles			
B(1)–O(1)–B(2)	121.8(3)	B(1)–O(2)–B(1) [a]	120.8(4)
O(1)–B(1)–O(2)	118.8(3)	O(1)–B(1)–C(1)	119.4(3)
O(2)–B(1)–C(1)	121.8(3)	O(1)–B(2)–O(1) [a]	117.9(4)
O(1)–B(2)–C(8)	121.1(2)	C(6)–C(1)–C(2)	116.7(3)
C(6)–C(1)–B(1)	122.9(3)	C(2)–C(1)–B(1)	120.3(3)
C(9)–C(8)–B(2)	121.4(2)		
Intermolecular contacts ≤ 3.40 Å			
O(1)···C(9) [b]	3.399(6)	B(1)···C(10) [b]	3.392(6)
B(1)···C(11) [c]	3.333(6)	B(2)···C(11) [d]	3.333(6)
B(2)···C(9) [c]	3.294(6)	B(2)···C(9) [b]	3.294(6)

Symmetry operations: [a] (1 − *x*, *y*, 0.5 − *z*); [b] (*x*, 1 − *y*, 0.5 + *z*); [c] (1 − *x*, 1 − *y*, − *z*); [d] (*x*, 1 − *y*, −0.5 + *z*).

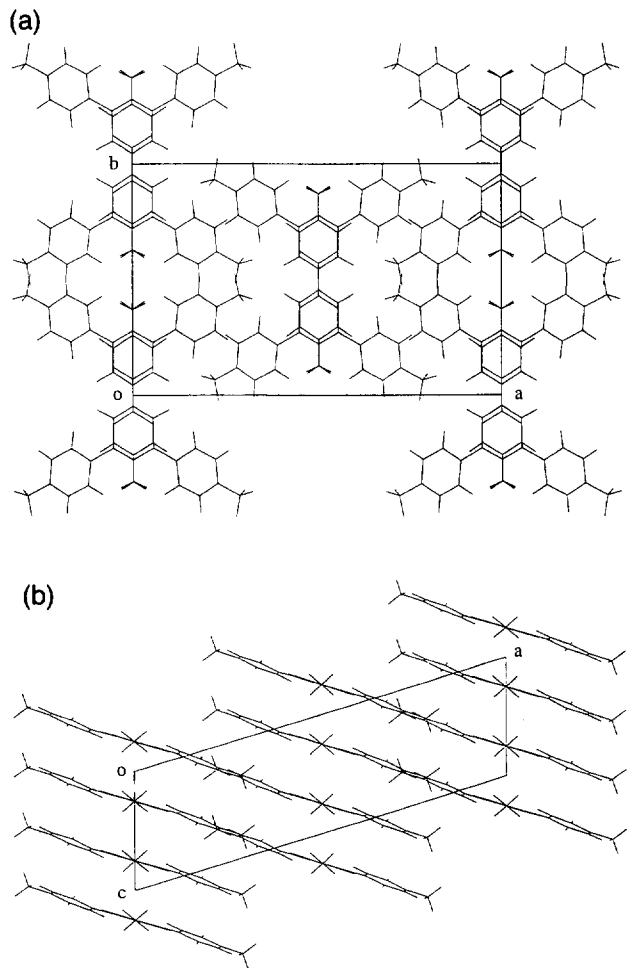

Fig. 2. Views along the (a) the *c* axis and (b) the *b* axis of the unit cell of (4-$MeC_6H_4)_3B_3O_3$ (**1**), showing intermolecular interactions.

and a packing diagram showing the layered structure **1** is shown in Fig. 2. The *p*-tolyl group of one molecule is able to sit above the boroxine ring of another molecule with the effect that each boron has at least one intermolecular interaction with a carbon atom at ca. 3.3 Å. Internuclear contacts of less than 3.4 Å are listed in Table 1 together with their unit cell symmetry operations. The intermolecular distances observed in **1** are comparable to those found in graphite (3.35 Å) and are clearly indicative of weak electronic intermolecular interactions. $Et_3B_3O_3$ has been reported to have a stacked structure with boroxine rings on top of one another with the intermolecular B · · · O interaction of 3.462 Å at −90 °C [8].

The molecular structure of the 4-picoline adduct $(4\text{-}MeC_6H_4)_3B_3O_3 \cdot 4$-picoline (**4**), has been determined by a single crystal X-ray diffraction study. Compound **4** has two independent molecules in the crystal which are shown in Fig. 3. Selected bond lengths and angles for both molecules are given in Table 2. Each molecule has a six-membered alternating B_3O_3 ring, similar to the starting boroxine ring system, but with an additional coordinate link from the nitrogen donor atom of the 4-picoline to one of the three boron atoms [B(3)] giving it a distorted tetrahedral geometry [bond angles at B(3) = 104.3(3)–115.4(4)°]. The remaining two boron atoms are three-coordinate and the three oxygen atoms are two-coordinate with bond angles about these annular atoms within the range 117.1(5)–123.1(4)°. The bond distances and angles about the 4-picoline substituents are basically as expected; however, the C–C–C angles at the carbon atoms [C(1), C(8) and C(15)] linked with the boron atoms are all significantly narrower [114.3(3)–116.1(5)°] than the ideal value 120° due to the linkage with boron. The B_3O_3 ring systems show significant deviations from planarity [atomic deviations of up to 0.117(4) and 0.038(3) Å from the respective least-squares planes for molecules 1 and 2 respectively] which may be explained by the tetrahedral geometry at B(3). The B–O distances within the rings also show interesting variations; those involving the three-coordinate boron atoms [B(1) and B(2)] are 1.337(6)–1.416(5), average 1.375 Å, whilst the corresponding values for the four-coordinate boron [B(3)] are ca. 0.09 Å longer at 1.439(6)–1.482(6) Å, average 1.467 Å. The same trend is observed for the C–C distances with values 1.510(6)–1.545(7) Å, average 1.524 Å, for B(1)/B(2) and 1.565(8), 1.588(8) Å, average 1.577 Å, for B(3). These differences are clearly due to the increased coordination number of B(3), which also results in the loss of π-bonding in the two B–O bonds involving this particular boron atom. A similar range and disposition of B–O bond lengths has been observed in the X-ray-determined structures of $2Ph_3B_3O_3 \cdot 3p\text{-}NH_2C_6H_4NH_2$ [3], $(4\text{-}MeC_6H_4)_3B_3O_3 \cdot C_6H_{11}NH_2$ [4] and $Ph_3B_3O_3 \cdot H_2NCH_2CH_2NMe_2$ [9]. The bond lengths and angles in

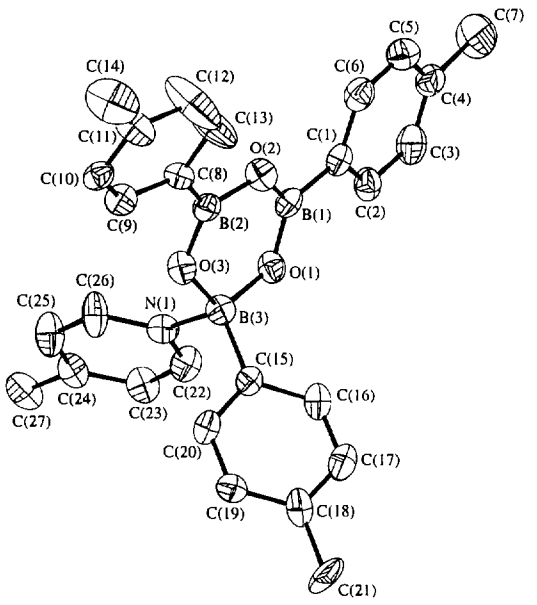

Molecule 1

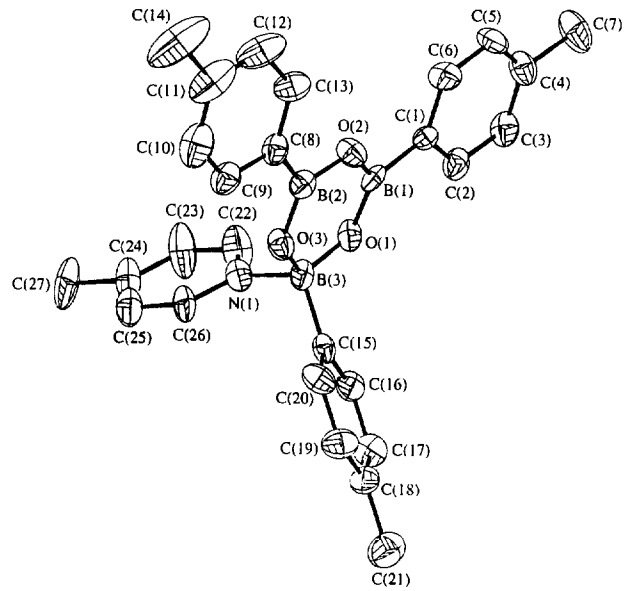

Molecule 2

Fig. 3. An ORTEP drawing of $4\text{-}MeC_5H_4N \cdot (4\text{-}MeC_6H_4)_3B_3O_3$ (**4**) showing the numbering scheme in the two independent molecules.

the 4-picoline species are as expected, but the two B(3)–N(1)–C(22)/C(26) angles are significantly different [116.7(5) vs. 125.6(4)° in molecule 1 and 119.3(3) vs. 124.0(5)° in molecule 2]. The much larger angles involving C(26) in molecule 1 and C(22) in molecule 2 can be explained by short intra-molecular non-bonded interactions O(3) · · · H(26) = 2.46(2) Å in molecule 1 and O(1) · · · H(22) = 2.38(2) Å in molecule 2, resulting from the particular orientations adopted by the 4-picoline groups. It is also important to mention that although

Table 2
Selected bond lengths (Å) and angles (deg) for $C_{27}H_{28}B_3NO_3$ (**4**)

	Molecule 1	Molecule 2
Bond lengths		
O(1)–B(1)	1.337(6)	1.340(6)
O(1)–B(3)	1.469(6)	1.477(6)
O(2)–B(1)	1.394(6)	1.389(6)
O(2)–B(2)	1.416(5)	1.399(7)
O(3)–B(2)	1.360(6)	1.361(7)
O(3)–B(3)	1.482(6)	1.439(6)
N(1)–B(3)	1.658(7)	1.637(6)
B(1)–C(1)	1.510(6)	1.545(7)
B(2)–C(8)	1.530(7)	1.512(7)
B(3)–C(15)	1.565(8)	1.588(8)
Bond angles		
B(1)–O(1)–B(3)	123.1(4)	122.2(4)
B(1)–O(2)–B(2)	120.8(4)	120.3(5)
B(2)–O(3)–B(3)	122.3(4)	123.0(5)
C(26)–N(1)–C(22)	117.6(5)	116.6(5)
C(22)–N(1)–B(3)	116.7(5)	124.0(5)
C(26)–N(1)–B(3)	125.6(4)	119.3(4)
O(1)–B(1)–O(2)	120.3(5)	120.7(5)
O(1)–B(1)–C(1)	121.8(5)	122.1(5)
O(2)–B(1)–C(1)	117.9(5)	117.1(5)
O(3)–B(2)–O(2)	118.1(5)	119.6(5)
O(3)–B(2)–C(8)	122.9(5)	122.3(6)
O(2)–B(2)–C(8)	119.0(5)	118.0(6)
O(1)–B(3)–O(3)	111.9(4)	113.7(5)
O(1)–B(3)–C(15)	114.4(5)	112.2(5)
O(3)–B(3)–C(15)	112.6(5)	112.5(5)
O(1)–B(3)–N(1)	104.3(4)	104.8(4)
O(3)–B(3)–N(1)	104.4(4)	105.6(4)
C(15)–B(3)–N(1)	108.3(4)	107.1(4)

the bond length and angle parameters in the two independent molecules of **4** are mutually comparable, they differ significantly in respect of the relative orientation of the *p*-tolyl and 4-picoline groups with the corresponding boroxine ring, which, respectively, have the values 62.7(9) and 56.1(9)° in molecule 1 and 51.7(8) and 63.0(9)° in molecule 2. Differences are also observed in the relative orientations of the *p*-tolyl rings at B(1) and B(2), as indicated by the values of the torsion angles O(2)–B(2)–C(8)–C(13) [−13.9(9)° for molecule 1 and 6.2(8)° for molecule 2] and O(1)–B(1)–C(1)–C(2) [2.3(9)° for molecule 1 and −8.6(7)° for molecule 2].

Preliminary results on the solid state ^{11}B–{^1H} MAS NMR of triarylboroxines and their Lewis base adducts have been reported [4]; these and some additional and some amended results are reported in Table 3. Shown in Fig. 4 are the solid state ^{11}B spectra of **1** and **9**. The spectrum of **9** (Fig. 4(a)) is typical of that of a Lewis base adduct of a triarylboroxine and the spectrum gave a reasonable fit to a simulation involving the superposition of two signals corresponding to two distinct boron environments being present. The normalized simulated components are shown in Fig. 5(a) and Fig. 5(b). The chemical shift from the observed spectra were 'corrected' for the effect of the quadrupolar interaction by comparison with the simulated spectra [10]. These 'corrected' chemical shifts (δ_{iso}) of the adducts are about +31 ppm and +4 ppm for the three- and four-coordinate boron atoms respectively, and they are similar to those observed in solution for analogous species. The spectrum of **1** (Fig. 4(b)) was very similar to that observed for **2** and was simulated (Fig. 5(c)) as one signal. Correction of chemical shifts leads to the value of +24.7 ppm and this is slightly upfield of that obtained in solution. A possible explanation of this high-field shift for **1** is that its solid state structure is layered (from X-ray diffraction studies, see above) and reveals that the B_3O_3 boroxine ring is sandwiched between two *p*-tolyl rings from neighbouring layers with B–C interactions of ca. 3.3 Å; such a geometry would increase electron density at boron with concomitant shielding of the boron nucleus. Previous reports on solid state ^{11}B–{^1H} MAS NMR have centred on differentiating between three-coordinate and four-coordinate boron atoms in crystalline borates and peroxyborates [11]. These

Table 3
Solid state ^{11}B MAS NMR data

	Isotropic shift δ_{iso} [a] (ppm)	Quadrupolar shift σ_{qs} [b] (ppm)	η	Quadrupolar coupling (Cq) (MHz)
1 (4-MeC_6H_4)$_3B_3O_3$	+24.7	−26.2	0.5	3.0
2 (3,5-$Me_2C_6H_3$)$_3B_3O_3$	+25.1	−26.2	0.5	3.0
5 (4-MeC_6H_4)$_3B_3O_3$ · cyclohexylamine	+31.7	−20.6	1.0	2.4
	+3.0	−7.0	0.5	1.6
6 (4-MeC_6H_4)$_3B_3O_3$ · isoquinoline	+32.5	−22.4	1.0	2.5
	+5.8	−6.8	0.6	1.5
7 (4-MeC_6H_4)$_3B_3O_3$ · benzylamine	+31.0	−20.6	1.0	2.4
	+1.9	−6.67	0.6	1.5
8 (3,5-$Me_2C_6H_3$)$_3B_3O_3$ · 4-picoline	+31.3	−20.6	1.0	2.4
	+4.8	−6.8	0.6	1.5
9 (3,5-$Me_2C_6H_3$)$_3B_3O_3$ · morpholine	+31.1	−20.6	1.0	2.4
	+3.3	−6.6	0.4	1.5

[a] $\delta_{iso} = \delta_{cg} - \sigma_{qs}$ (δ_{cg} is the centre of gravity chemical shift of the observed signal) [10].
[b] $\sigma_{qs} = \nu_{CG} - \nu_L = -10^6(Cq)^2(1 + 0.33\eta^2)/40(\nu_L)^2$ (ν_L = 96.234 MHz) [10].

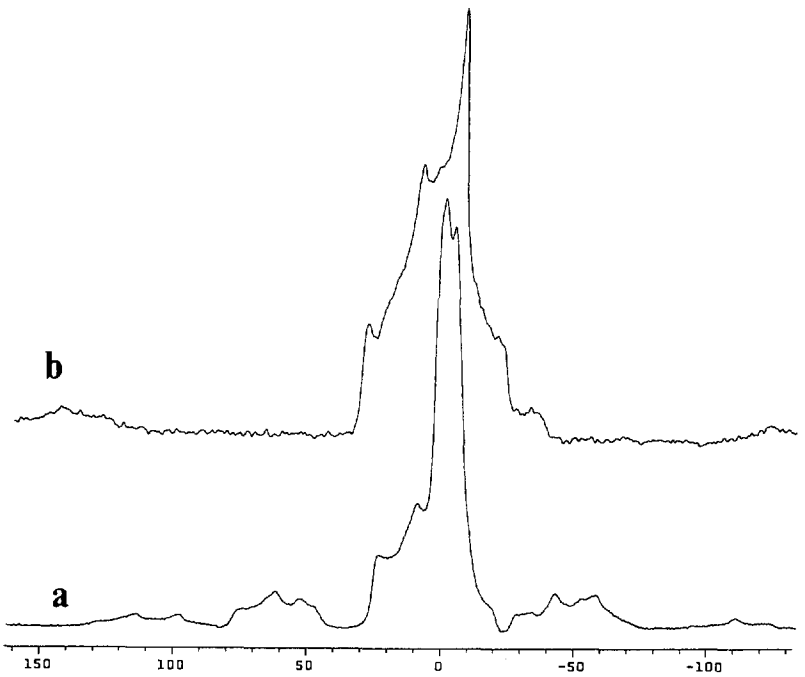

Fig. 4. Solid state $^{11}B-\{^1H\}$ MAS NMR spectra of (a) $(3,5\text{-}Me_2C_6H_3)_3B_3O_3 \cdot$ morpholine (**9**) and (b) $(4\text{-}MeC_6H_4)_3B_3O_3$ (**1**). Spectra were recorded at ambient temperature at 96.234 MHz with a relaxation delay of 1.0 s, pulse angles of 20° and spin rates of 5000 Hz and 12 800 Hz for (a) and (b) respectively. Chemical shifts are relative to $BF_3 \cdot OEt_2$.

spectra illustrate the usefulness of $^{11}B-\{^1H\}$ MAS NMR with respect to molecular solids and also clearly warn that intermolecular solid state interactions may unexpectedly effect corrected chemical shift values.

2.2. Synthesis and characterization of 3 and its 1:1 amine adducts

$(2\text{-}MeC_6H_4)_3B_3O_3$ (**3**) was conveniently prepared by the literature method [12] used for **1** and **2**. The synthesis of 1:1 amine adducts (**10–16**) of the triarylboroxine **3** were relatively straightforward [2] and proceeded in near quantitative yield in Et_2O at room temperature according to Eq. (1) (L = 4-picoline, cyclohexylamine, pyridine, 3-picoline, piperidine, isoquinoline, and benzylamine). We were unable to prepare adducts of the ligands morpholine and tributylamine with **3** and this we attribute to destabilizing steric interactions. Eq. (1) can be considered as an equilibrium reaction and product formation would result in a reduction of participating species with a resulting decrease in entropy. Unless the reaction is sufficiently exothermic

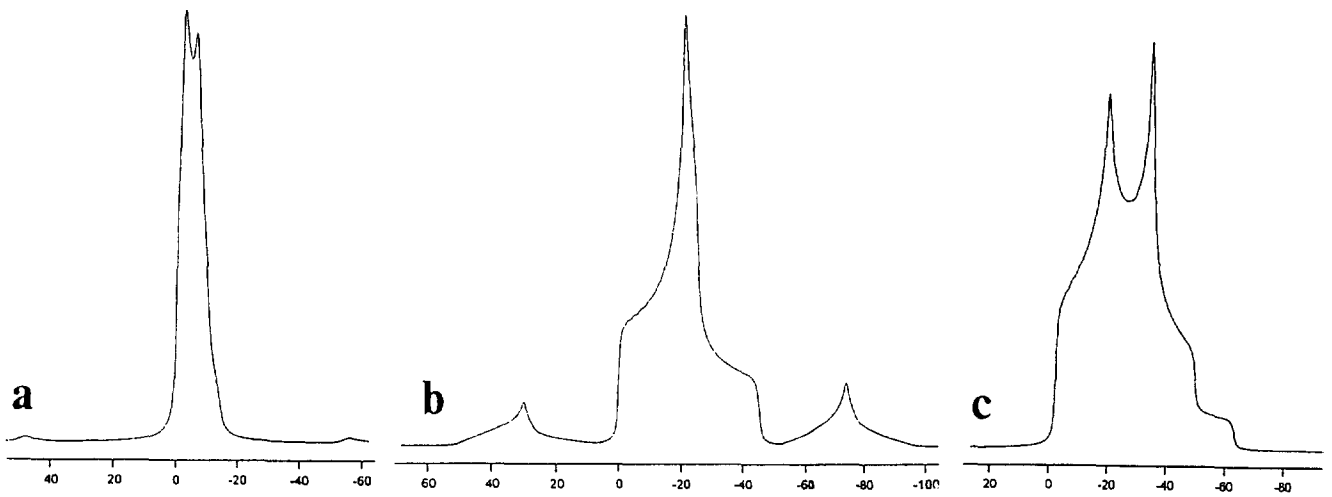

Fig. 5. Simulated solid state $^{11}B-\{^1H\}$ MAS NMR spectra for (a) four-coordinate signal of $(3,5\text{-}Me_2C_6H_3)_3B_3O_3 \cdot$ morpholine (**9**) and (b) three-coordinate signal of $(3,5\text{-}Me_2C_6H_3)_3B_3O_3 \cdot$ morpholine (**9**), and (c) $(4\text{-}MeC_6H_4)_3B_3O_3$ (**1**). Parameters varied in the simulations were the asymmetry factor η and quadrupolar coupling (Cq) and values used are given in Table 3.

Table 4
Analytical [a] and physical data for 1:1 amine:(2-$MeC_6H_4)_3B_3O_3$ adducts

Complex	Yield (%)	M.p. (°C)	Analysis (%)		
			C	H	N
10 4-picoline · **3**	88	128–130	72.7 (72.6)	6.1 (6.3)	3.0 (3.1)
11 cyclohexylamine · **3**	85	83–85	71.3 (71.6)	8.2 (7.6)	3.1 (3.1)
12 pyridine · **3**	93	128–130	72.1 (72.1)	6.0 (6.1)	3.2 (3.2)
13 3-picoline · **3**	87	115–118	72.8 (72.6)	6.6 (6.3)	3.1 (3.1)
14 piperidine · **3**	88	85–87	71.7 (71.4)	7.5 (7.3)	3.2 (3.2)
15 isoquinoline · **3**	91	127–129	74.5 (74.9)	5.5 (5.9)	2.7 (2.9)
16 benzylamine · **3**	90	117–118	73.5 (73.0)	7.0 (6.6)	3.0 (3.0)

[a] Required amounts given in parentheses.

to counterbalance this then the equilibrium will favour the starting materials. For most of the ligands described above ΔH is sufficiently negative and the reactions are observed to go to completion. However, steric interactions [13] will reduce the magnitude of ΔH with the consequence that for the sterically demanding ligands product formation will not be favoured.

$$L + (2\text{-}MeC_6H_5)_3B_3O_3 = (2\text{-}MeC_6H_5)_3B_3O_3 \cdot L \quad (1)$$

All isolated compounds gave satisfactory elemental analysis, were air-stable white crystalline solids with clearly defined melting points (Table 4), and were readily soluble in chlorinated and aromatic solvents but less soluble in Et_2O and petroleum ether. Compounds **10–16** were characterized by ^1H and ^{13}C NMR spectroscopy and by IR spectroscopy. IR spectra of compounds **10–16** (Table 5) all show very strong bands associated with B–O stretches in the region 1450–1250 cm^{-1} but are not otherwise noteworthy [1].

Table 5
Spectroscopic (^1H, ^{13}C NMR [a] and IR [b]) data for 1:1 amine:(2-$MeC_6H_4)_3B_3O_3$ adducts

Complex	Data
10	$\delta(^1H)$: 8.65 (d, 2H), 8.05 (d, 3H), 7.0–7.2 (m, 11H), 2.6 (s, 9H), 2.3 (s, 3H). $\delta(^{13}C)$: 156.34, 144.36, 143.50, 135.68, 130.14, 129.91, 126.12, 124.82, 22.75, 20.29. IR: 3214 (br), 3054, 3014, 2925, 2260, 1630, 1598, 1567, 1442, 1395 (br, vs), 1300, 1276 (br, vs), 1240, 1197, 1130, 1078, 1024, 976, 876, 850, 816, 786, 746, 733, 688, 642.
11	$\delta(^1H)$: 8.1 (d, 3H), 7.1–7.4 (m, 9H), 4.2 (s, 2H), 2.6 (s, 9H), 2.5 (s, 1H), 1.8 (s, 2H), 1.5 (s,3H), 1.1 (s, 5H). $\delta(^{13}C)$: 156.34, 143.65, 135.40, 130.13, 129.66, 124.89, 50.49, 32.16, 24.54, 24.15, 22.79. IR: 3320 (br), 3052, 2935, 2859, 2361, 1598, 1567, 1522, 1448, 1385 (br, vs), 1276 (br, vs), 1163, 1130, 1086, 1045, 811, 759, 735, 685.
12	$\delta(^1H)$: 8.9 (d, 2H), 8.15 (d, 3H), 8.0 (t, 1H), 7.6 (t, 2H), 7.2–7.3 (m, 9H), 2.6 (s, 9H). $\delta(^13C)$: 144.91, 144.00, 135.41, 130.12, 129.57, 125.24, 124.81, 22.71. IR: 3220 (br), 3049, 2923, 1619, 1599, 1560, 1508, 1458, 1388 (br, vs), 1278 (br, vs), 1196, 1136, 1081, 1050, 1030, 979, 872, 834, 802, 776, 746, 728, 691, 674, 628.
13	$\delta(^1H)$: 8.8 (s, 2H), 8.2 (d, 3H), 7.75 (d, 1H), 7.0–7.4 (m, 11H), 2.7 (s, 9H), 2.45 (s, 3H). $\delta(^{13}C)$: 156.36, 144.53, 144.00, 141.86, 141.25, 135.80, 135.40, 130.08, 129.51, 124.78, 22.71, 18.81. IR: 3213 (br), 3054, 3015, 2924, 1926, 1622, 1458, 1567, 1444, 1389 (br, vs), 1325, 1278 (br, vs), 1245, 1071, 1031, 1110, 1080, 1040, 1025, 977, 946, 855, 826, 788, 745, 692, 674, 656.
14	$\delta(^1H)$: 8.05 (d, 3H), 7.2–7.3 (m, 9H), 3.05 (m, 3H), 2.8 (s, 9H), 1.7 (s, 6H), 1.3 (m, 2H). $\delta(^{13}C)$: 143.55, 135.58, 130.13, 129.42, 124.83, 45.21, 25.40, 23.06, 22.94. IR: 3260 (br), 3051, 3009, 2926, 2860, 1598, 1448, 1376 (br, vs), 1275 (br, vs), 1198, 1173, 1130, 1086, 1043, 978, 813, 753, 683.
15	$\delta(^1H)$: 9.5 (s, 1H), 8.6 (d, 1H), 8.1 (d, 4H), 7.85 (m, 3H), 7.7 (m, 1H), 7.2 (m, 9H), 2.6 (s, 9H). $\delta(^{13}C)$: 147.90, 144.06, 136.97, 136.27, 135.47, 134.08, 130.19, 129.56, 129.38, 127.65, 126.72, 124.82, 123.23, 22.76. IR: 3216 (br), 3056, 2926, 1642, 1597, 1566, 1445, 1388 (br, vs), 1323, 1278 (br, vs), 1241, 1198, 1177, 1131, 1112, 1093, 1060, 1025, 977, 851, 822, 767, 748, 689.
16	$\delta(^1H)$: 8.1 (d, 3H), 7.0–7.4 (m, 14H), 4.0 (s, 2H), 2.75 (s, 9H), 2.5 (s, 2H) $\delta(^{13}C)$: 156.36, 143.66, 136.38, 135.52, 130.20, 129.77, 129.42, 128.74, 127.96, 124.95, 45.07, 22.86. IR: 3415 (br), 3294, 3099, 2959, 1597, 1483, 1451, 1370 (br, vs), 1308, 1274 (br, vs), 1252, 1189, 1132, 1088, 1058, 1028, 1008, 958, 923, 849, 771, 752, 734, 698, 682, 632.

[a] In $CDCl_3$ solution at room temperature.
[b] KBr pellets (cm^{-1}); medium intensity unless otherwise stated.

Table 6
Variable-temperature NMR data

Complex	T_c (K) [a]	$\delta\nu$ (Hz) [a]	k (s^{-1}) [b]	$\Delta G^{\ddagger}$ (kJ mol^{-1}) [c]
10	230	135	300	44.9
11	233	18	40	49.4
15	230	125	278	45.1
16	208	23	51	43.5

[a] From methyl resonances of the $(2\text{-}MeC_6H_4)_3B_3O_3$ (**3**).
[b] $k = 2^{-1/2}\pi\delta\nu$.
[c] $\Delta G^{\ddagger} = -RT\ln(khk_B^{-1}T^{-1})$.

2.3. Solution NMR studies on 1:1 amine adducts of 3

The ^1H and ^{13}C spectra recorded at room temperature for adducts **10–16** are reported in Table 5. The data clearly show the equivalence of the methyl substituents on the boroxine aryl rings demonstrating that at room temperature the three boron centres of the boroxine · ligand adduct are equivalent. These results are in accord with those obtained [2] for various $Ph_3B_3O_3 \cdot L$ adducts and consistent with a rapid ligand dissociation–recombination exchange process occurring as has been proposed for adducts of **1** and **2** [4]. Compounds **10–16** showed temperature-dependent ^1H spectra and for **10**, **11**, **15**, and **16** the low temperature (−90 °C) spectra displayed two signals (relative intensity 2:1) for the *o*-tolyl methyl groups consistent with slow ligand-exchange as has been observed for adducts of **1** and **2** [4]. These signals coalesced to singlets as the samples were warmed. $\Delta G^{\ddagger}$ for the various ligand exchange processes were calculated from the Eyring equation using the exchange rate k at coalescence temperature derived from the separation of signals at slow-exchange [14,15]. Complexes **12**, **13**, and **14** showed similar behaviour but we were unable to obtain limiting slow-exchange spectra. Experimental and calculated data are recorded in Table 6 with the $\Delta G^{\ddagger}$ values for compounds **10**, **11**, **15** and **16** spanning the range 43.5–49.4 kJ mol^{-1}. Data for complexes of **3** are compared in Table 7 with literature data [4] for the corresponding complexes of **1** and **2**. We were interested to see if increasing the steric demands of the arylboroxine would lead to an increase in $\Delta G^{\ddagger}$ for the ligand dissociation–recombination process. The results suggest that this is so for cyclohexylamine and isoquinoline but not so for benzylamine. The situation is not clear-cut and steric congestion, although playing a significant role, is clearly not the dominating factor in all cases. However, since the differences in $\Delta G^{\ddagger}$ are small and values are probably only reliable to within 1–2 kJ mol^{-1} caution must be exercised in interpreting the available data. It is possible that since the $\Delta G^{\ddagger}$ values are generally similar that the dominant factor may be attributed to the disruption of the π-bonding in the B_3O_3 ring system upon adduct formation. Attempts to obtain ^{11}B spectra of compounds **10–16** at room temperature were unsuccessful.

3. Experimental

3.1. General

Reactions were carried out by standard Schlenk techniques under N_2 and all solvents were dried before use. IR spectra were recorded on a Perkin–Elmer FT-IR 1600 spectrometer as KBr discs. Multi-element solution NMR spectra were recorded on a Bruker AC CP/MAS NMR spectrometer operating at 250 MHz for ^1H and 62.9 MHz for $^{13}C\text{-}\{^1H\}$. Chemical shifts (δ) are given in parts per million with positive values towards high frequency (downfield) from $SiMe_4$. $(2\text{-}MeC_6H_4)_3B_3O_3$ was prepared from $1,2\text{-}MeC_6H_4Br$ by adaption of published methods [12]. The amines were obtained commercially and were distilled immediately before use. The complexes **10–16** were all prepared by the same method [2,4] as detailed below for **10**. Analytical data and yields can be found in Table 4. ^1H and ^{13}C NMR data and IR data are given in Table 5. Compound **4** was prepared as in Ref. [4] and crystals of it and compound **1** suitable for X-ray diffraction study were grown by diffusion of 40–60 °C petroleum ether into a layered solution of the complex in $CHCl_3$.

3.2. Preparation of $4\text{-}MeC_5H_4N \cdot (2\text{-}MeC_6H_4)_3B_3O_3$ (10)

4-Picoline (0.264 g, 2.83 mmol) in Et_2O (10 cm^3) was added to a stirred suspension of $(2\text{-}MeC_6H_4)_3B_3O_3$ (1.0 g, 2.83 mmol) in Et_2O (10 cm^3) at room temperature. The suspension of the triarylboroxine dissolved after a few minutes stirring and the resulting solution was filtered. The solution was reduced in volume to

Table 7
Comparison of $\Delta G^{\ddagger}$ values for amine complexes of $(4\text{-}MeC_6H_4)_3B_3O_3$ (**1**), $(3,5\text{-}Me_2C_6H_3)_3B_3O_3$ (**2**), and $(2\text{-}MeC_6H_4)_3B_3O_3$ (**3**)

	$4\text{-}MeC_5H_4N$	Isoquinoline	$PhCH_2NH_2$	$C_6H_{11}NH_2$	Morpholine
$(4\text{-}MeC_6H_4)_3B_3O_3$ (**1**) [a]	—	43.8	46.2	43.1	44.1
$(3,5\text{-}Me_2C_6H_3)_3B_3O_3$ (**2**) [a]	—	45.4	47.8	47.3	49.3
$(2\text{-}MeC_6H_4)_3B_3O_3$ (**3**) [b]	44.9	45.1	43.5	49.4	—

[a] Data from Ref. [4].
[b] This work.

Table 8
Crystal data and details of data collection and structure refinement for $C_{21}H_{21}B_3O_3$ (1) and $C_{27}H_{28}B_3NO_3$ (4) [a]

Compound	(1)	(4)
Formula	$C_{21}H_{21}B_3O_3$	$C_{27}H_{28}B_3NO_3$
M.W.	353.81	446.93
Crystal system	Monoclinic	Triclinic
a/Å	22.591(6)	11.8570(10)
b/Å	13.269(4)	14.483(3)
c/Å	6.8389(10)	15.527(2)
α/deg	90	78.530(12)
β/deg	106.82(2)	88.000(10)
γ/deg	90	78.850(13)
V/Å^3	1962.4(8)	2563.8(6)
Space group	$C2/c$ (No. 15)	$P\bar{1}$ (No. 2)
Z	4	4
T/K	150	293
D_c/g cm^{-3}	1.198	1.158
$F(000)$	744	944
μ(Mo Kα)/cm^{-1}	0.76	0.73
Crystal size/mm^3	0.28 × 0.16 × 0.12	0.16 × 0.12 × 0.10
θ range data collection/deg	1.80–24.98	1.75–25.16
h_{min}, h_{max}	−25, 26	−13, 10
k_{min}, k_{max}	−13, 14	−16, 15
l_{min}, l_{max}	−7, 5	−16, 17
Total data measured	3986	9775
Total unique (R_{int})	1483 (0.0670)	6544 (0.0870)
Refinement method	Full-matrix least squares on F^2	
No. of parameters/data	169/1483	621/6544
ρ_{min}, ρ_{max}/e$^-$ Å^{-3}	−0.205, +0.260	−0.132, +0.126
$(\Delta/\sigma)_{max}$	0.002	0.001
Goodness-of-fit	0.871	0.456
R_1	0.0982 (0.0502) [b]	0.1811 (0.0443) [b]
wR_2	0.1265 (0.1167) [b]	0.0789 (0.0616) [b]

[a] Details in common: fast area detector diffractometer, Mo Kα radiation, $\lambda = 0.71069$ Å.
[b] The R values for data with $I > 2\sigma(I)$ [751 for (1) and 1579 for (4)] are given in parentheses. $R_1 = \Sigma(F_o - F_c)/\Sigma(F_o)$; $wR_2 = \{\Sigma[w(F_o^2 - F_c^2)^2]/\Sigma[w(F_o^2)^2]\}^{1/2}$; $w = 1/[(\sigma^2(F_o^2) + (0.0525P)^2]$, where $P = [\text{Max}(F_o^2) + 2F_c^2]/3$, for (1) and 0.0 for (4).

dryness and the product (1.11 g, 88%) was obtained, after oven drying (100 °C, 4 h) as a white air-stable analytically pure solid (m.p. 128–130 °C).

3.3. X-ray structures of (4-MeC$_6$H$_4$)$_3$B$_3$O$_3$ (1) and 4-MeC$_5$H$_4$N · (4-MeC$_6$H$_4$)$_3$B$_3$O$_3$ (4)

All crystallographic measurements were made using a FAST area detector diffractometer and Mo Kα radiation ($\lambda = 0.71069$ Å), following previously described procedures [16]. The structures were solved by direct methods (SHELXS86) [17] and refined on F^2 by full-matrix least squares (SHELXL93) [18] using all unique data to final $wR = 0.1265$ (on F^2) (all 1483 data and 169 parameters) for compound (1) and 0.0789 (all 6544 data and 621 parameters) for (4); the R-values [on F, $F_o > 4\sigma(F_o)$] were 0.0502 for compound (1) and 0.0443 for compound (4). In both structures, the non-hydrogen atoms were refined anisotropically. In (1) the hydrogen atoms were experimentally located and isotropically refined. For (4) these were included in calculated posi-

Table 9
Atomic coordinates (× 10^4) and equivalent isotropic displacement parameters (Å^2 × 10^3) for $C_{21}H_{21}B_3O_3$ (1)

	x	y	z	U_{eq} [a]
O(1)	4472(1)	6235(1)	1525(3)	32(1)
O(2)	5000 [b]	7793(2)	2500 [b]	30(1)
B(1)	4464(2)	7277(2)	1516(5)	26(1)
B(2)	5000 [b]	5697(4)	2500 [b]	24(1)
C(1)	3863(1)	7835(2)	383(4)	30(1)
C(2)	3359(2)	7300(3)	−885(5)	37(1)
C(3)	2824(2)	7780(3)	−1948(5)	41(1)
C(4)	2764(1)	8813(3)	−1862(5)	39(1)
C(5)	3257(2)	9354(3)	−625(5)	48(1)
C(6)	3794(2)	8878(3)	490(5)	40(1)
C(7)	2175(2)	9339(4)	−3032(7)	62(1)
C(8)	5000 [b]	4551(3)	2500 [b]	26(1)
C(9)	4470(2)	4000(2)	1471(4)	33(1)
C(10)	4476(2)	2948(3)	1468(5)	38(1)
C(11)	5000 [b]	2410(3)	2500 [b]	39(1)
C(12)	5000 [b]	1274(4)	2500 [b]	57(2)

[a] U_{eq} is defined as one-third of the trace of the orthogonalized U_{ij} tensor.
[b] Invariant parameters due to site symmetry restrictions.

tions (riding model) with U_{iso} set at 1.2 (CH) or 1.5 (CH_3) times the U_{eq} of the parent atom. The crystal data and details of data collection and structure refinement for both compounds are presented in Table 8. The non-hydrogen atomic parameters for (1) are given in Table 9. The anisotropic displacement coefficients, hydrogen atom parameters and full lists of bond lengths and angles have been deposited as supplementary material.

Acknowledgements

We thank Dr. D. Apperley at the EPSRC solid state NMR service centre (Durham University) for spectra and advice, and also the crystallographic referee for helpful comments.

References

[1] H.R. Snyder, M.S. Konecky and W.J. Lennarz, *J. Am. Chem. Soc., 80* (1958) 3611.
[2] J.M. Ritchey, Synthesis and properties of addition complexes of boroxines and other selected boron-containing systems, *Ph.D. Thesis*, University of Colorado, 1968.
[3] M. Yalpani and R. Boese, *Chem. Ber., 116* (1983) 3347.
[4] M.A. Beckett, G.C. Strickland, K.S. Varma, D.E. Hibbs, M.B. Hursthouse and K.M.A. Malik, *Polyhedron, 14* (1995) 2623.
[5] W.L. Fielder, M.M. Chamberlain and C.H. Brown, *J. Org. Chem., 26* (1961) 2154.
[6] A. Burg, *J. Am. Chem. Soc., 62* (1940) 2228.
[7] C.P. Brock, R.P. Minton and K. Niedenzu, *Acta. Crystallogr. Sect. C:, 43* (1987) 1775.
[8] R. Boese, M. Palk and D. Blaser, *Angew. Chem. Int. Ed. Engl., 26* (1987) 245.
[9] G. Furguson, A.J. Lough, J.P. Sheehan and T.R. Spalding, *Acta Crystallogr. Sect. C:, 46* (1990) 2390.
[10] G. Engelhardt and D. Michel, *High Resolution Solid-State NMR of Silicates and Zeolites*, Wiley, New York, 1987.
[11] D. Muller, A.R. Grimmer, U. Timper, G. Heller and M. Shakibaie-Moghadam, *Z. Anorg. Allg. Chem., 619* (1993) 1262.
[12] R.M. Washburn, E. Levens, C. Albright and F. Billig, *Org. Synth., 39* (1959) 3.
[13] H.C. Brown, *J. Chem. Soc.*, (1956) 1248.
[14] H.S. Gutowsky and C.H. Holm, *J. Chem. Phys., 25* (1956) 1228.
[15] C.E. Holloway, G. Hulleey, B.F.G. Johnson and J. Lewis, *J. Chem. Soc. A:*, (1966) 53.
[16] J.A. Darr, S.R. Drake, M.B. Hursthouse and K.M.A. Malik, *Inorg. Chem., 32* (1993) 5704.
[17] G.M. Sheldrick, *Acta Crystallogr. Sect. A:, 46* (1990) 467.
[18] G.M. Sheldrick, SHELXL93, *Program for Crystal Structure Refinement*, University of Gottingen, Germany, 1993.